Title	Novel neural network model of power amplifier plus Iq imbalances
Author(s)	Fu, Kai; Law, Choi Look; Thein, Than Tun
Citation	Fu, K., Law, C. L., & Thein, T. T. (2013). Novel Neural Network Model Of Power Amplifier Plus Iq Imbalances. Progress In Electromagnetics Research B, 46, 177-192.
Date	2013
URL	http://hdl.handle.net/10220/18449
Rights	

Progress In Electromagnetics Research B, Vol. 46, 177–192, 2013

NOVEL NEURAL NETWORK MODEL OF POWER AMPLIFIER PLUS IQ IMBALANCES

Kai Fu*, Choi Look Law, and Than Tun Thein

School of EEE, Nanyang Technological University, 50 Nanyang Avenue, Singapore 639798, Singapore

Abstract—Traditionally, the transmitter (TX) IQ imbalances distortion and power amplifier (PA) distortion are separately modeled. In this paper, the behavior of the two distortions are unified, and characterized by a single model. Rectangular structured Focused Time-Delay Neural Network (RSFTDNN) is proposed to uniformly model IQ imbalances and PA distortions. As a result, the physical distortions in the analog circuits are further abstracted. It also saves computation resources in simulation. Unlike the polynomial based model, which suffers from condition number effects and inaccuracy for deeply nonlinear system, the proposed RSFTDNN shows high accuracy. Two cases of real experiments are carried out, where RSFTDNN model shows much better performance than the polynomial based model in the sense of model accuracy.

1. INTRODUCTION

Modern wireless communication systems suffer from severe signal distortion at the power amplifier and IQ imbalance distortion in the modulator/up converter. The Power amplifier (PA) [1] shows nonlinear [2] and memory distortion [3, 4]. And the memory or frequency-dependent effects become much more significant and influential [5] when the transmitted signal is a wideband signal, e.g., Orthogonal Frequency Division Multiplexing (OFDM) based signals [4]. Due to its peculiarity of a high Peak-to-Average Power Ratio (PAPR) [6], OFDM-based signals (WLAN and LTE signals) are very sensitive to the PA nonlinear distortions. Another important distortion is TX IQ imbalances [7, 8], represented by the gain imbalance between I and Q paths, and the shift from the ideal phase difference

Received 24 August 2012, Accepted 26 November 2012, Scheduled 29 November 2012
* Corresponding author: Kai Fu (fu0001ai@ntu.edu.sg).

between the two local oscillators (LOs). TX IQ imbalances are also frequency-dependent with wideband [7] signals. The TX IQ imbalances distortion may introduce Mirror Frequency Interference (MFI) [8].

Behavioral models of these physical distortions are usually used in simulation — a critical step to analyze the influence and find a way to compensate it. Traditionally, power amplifier and TX IQ imbalances are simulated separately by two totally independent behavioral models. This approach increases the cost of resources. Moreover, it is very difficult to design and setup the experiment to separately identify both models — the power amplifier and other RF devices are often implemented in a circuit board, or even in a chip, rendering it very difficult to totally separate one from the other and identify the corresponding models independently.

Recently, some polynomial based models [9] have been proposed to treat PA distortion and TX IQ imbalances in a single unified model. However, polynomial based models can only model mild nonlinear system [10], because it is difficult to accurately identify the coefficients with very high nonlinear order, owing to the condition number problem [11]. In [12], real-valued focused time-delay neural network (RVFTDNN) is used to predistort PA nonlinear impairments. However, it does not discuss the influence of IQ imbalances, nor does it discuss the issue of condition number problem. In this paper, the power amplifier and TX IQ Imbalances distortions are treated as a single black box, and modeled in one behavioral model — Rectangular structured Focused Time-Delay Neural Network (RSFTDNN). Here the advantages of RSFTDNN are: (1) It provides a unified view of the impairments of the transmitter. (2) It can avoid the condition number problem of the polynomial based models, and accurately characterize a deeply nonlinear communication system. (3) The network structure is simple, and easy to be implemented, and it can save computation resources in the simulation.

The proposed model is designed and specified according to the characteristics of power amplifier and TX architecture. The proposed neural network is double input (real part and imaginary part separately) and single output (complex-valued). In order to model the "bend-down" AM/AM characteristics of a power amplifier, the activation function should be saturated for large input. And to model the memory effects, the proposed neural network uses both the current and the past inputs. Furthermore, condition number problem on polynomial based model is also discussed and analyzed. An experiment setup is specifically designed to avoid additional RX IQ imbalances interference, and a processing method is used to achieve accurate time-alignment of the input and output signals.

The structure of the paper is arranged as follows: Section 2 firstly illustrates the scheme of uniformly modeling the PA distortion and IQ imbalances, and then analyzes the limitation of condition number problem on polynomial based models. Section 3 proposes and analyzes the RSFTDNN model. Section 4 shows the experiment results. Finally, Section 5 gives the conclusion.

2. UNIFIED MODEL ON PA AND IQ IMBALANCES

2.1. Unified Model

The overall diagram of a typical wireless transmitter is shown in Figure 1. The distortion of TX IQ imbalances models the impairments or difference between $s(n)$ and $x_l(n)$ (digitized version of $x_l(t)$); and the distortion of the power amplifier models the impairments or difference between $x_l(n)$ and $y_l(n)$ (digitized version of $y_l(t)$). Traditionally, these two distortions are modeled and simulated separately by two independent models. One possible reason for treating these two distortions separately may be that they are caused by two different physical mechanisms. However, from the viewpoint of system-level simulation, all the underneath physical characteristics are ignored, while only the output signals of concern. Hence it is natural and

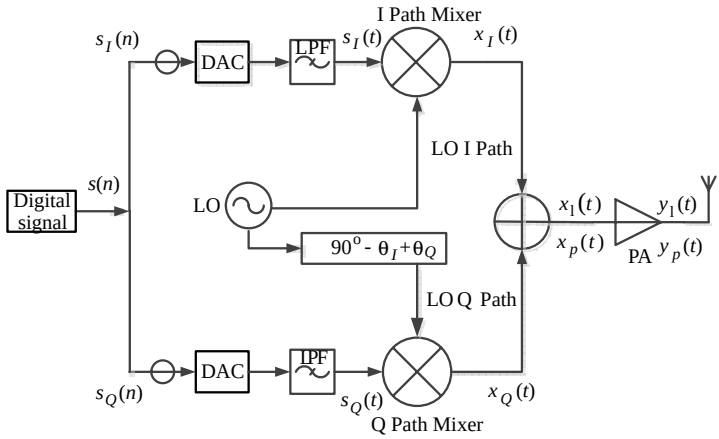

Figure 1. Overall diagram of a wireless transmitter: The signal with the subscript p is the RF pass-band signal with carrier frequency, while the signal with the subscript l is the corresponding low-pass equivalent signal. The index n means the digitized signal, while index t means the continuous analog signal after DAC.

sensible to merge these two distortions into one unified black box, using one mathematical equation to model the relationship between its input $s(n)$ and output $y_l(n)$. This saves the computation resources, and represents a unified view of the transmitter impairments.

2.2. Model Choice and Limitation on Polynomial Based Models

Polynomial based models and neural network models are two general classes of models, which can be used to characterize the behavior of a system. The class of polynomial based models can only model mildly nonlinear system [10], because it is difficult to accurately identify the coefficients with very high nonlinear order. This is due to the fact that the condition number increases very quickly with increasing nonlinear order. A large condition number means inaccurate identification results as demonstrated in the derivation below.

One important character of polynomial based model is that the output of the model is in linear relationship with the coefficients. Hence usually the way to identify the coefficients is to solve the linear equation:

$$\mathbf{A}\mathbf{x} \simeq \mathbf{b} \tag{1}$$

where the matrix $\mathbf{A}$ contains all the linear and nonlinear orders of the input samples, vector $\mathbf{b}$ is the output samples, and the vector variable $\mathbf{x}$ is the coefficients to be identified. Usually, the number of samples is much larger than the number of coefficients, resulting in a least squares (LS) problem.

For rectangular matrix $\mathbf{A}_{N\times L}$, where $N > L$, the condition number is defined

$$\chi(\mathbf{A}) = \|\mathbf{A}\|_{\mathbf{2}} \cdot \left\|\mathbf{A}^{\dagger}\right\|_{\mathbf{2}} = \frac{\sigma_{\max}}{\sigma_{\min}} \tag{2}$$

where $\{\sigma_i\}_L$ is the singular values of $\mathbf{A}_{N\times L}$ and $\|\mathbf{A}\|_{\mathbf{2}}$ the 2-norm of matrix $\mathbf{A}$.

The angle between the m-dimensional vector $\mathbf{b}$ and the space $span(\mathbf{A})$ is defined

$$\cos\theta = \frac{\|\mathbf{A}\mathbf{x}\|_2}{\|\mathbf{b}\|_2} \tag{3}$$

where $\mathbf{x}$ is the least squares solution.

Theorem 1. *For full column rank $N \times L$ matrix $\mathbf{A}$, and if the noise is only present in vector $\mathbf{b}$, the upper boundary of the sensitivity of the LS solution is calculated [13] as:*

$$\frac{\|\mathbf{\Delta x}\|_{\mathbf{2}}}{\|\mathbf{x}\|_{\mathbf{2}}} \leq \frac{\chi(\mathbf{A})}{\cos\theta} \frac{\|\mathbf{\Delta b}\|_{\mathbf{2}}}{\|\mathbf{b}\|_{\mathbf{2}}} \tag{4}$$

Proof. The proof is also given in [13].

Equation (4) prevails in all the polynomial models that have linear relationship between their outputs and their coefficients. It shows that the error in the coefficients $\mathbf{x}$ is highly correlated to the condition number $\chi(\mathbf{A})$, with its upper boundary being linearly proportional to the condition number.

On the contrary, neural network is good at modeling even a highly nonlinear system. With a proper number of layers and neurons, the neural network can characterize a system with arbitrary accuracy [14]. Neural network has no such limitation as condition number in polynomial based models that may set an upper boundary for the performance and accuracy. Furthermore, from Figure 1, it is clear that to characterize TX IQ imbalances and PA distortions together, the model should have double inputs (real $s_I(n)$ and imaginary $s_Q(n)$, respectively). However, the classical polynomial model is accustomed to model single input single output (SISO) system, and hence some modification or extension are necessary to model such double input system, which may very well increase the complexity and computation cost. On the contrary, neural network has natural flexibility in the number of inputs and outputs, and can model such double input system quite straightforwardly. Last but not least, neural network enjoys more freedom: i.e., it can accommodate varying number of layers or neurons in each layer, changes in the type of activation function, or even changes in the connections or structure. Hence, neural network may be a better choice to model the unified system consisting of TX IQ imbalances and highly nonlinear PA.

3. PROPOSED NEURAL NETWORK MODEL

The relationship between the transmitted baseband signal $s(n)$ and the lowpass equivalent front end signal $y_l(n)$ shown in Figure 1 models the IQ imbalances and PA distortions. The model should be a double-input model because TX IQ imbalances distortion results in different impairments to the real and imaginary parts of $s(n)$. Taking memory effects into consideration, the model can be generalized as:

$$\begin{aligned} y_l(n) &= f\left(\mathbf{s}_I(n), \mathbf{s}_Q(n)\right) \\ &= f\left(s_I(n), \ldots, s_I(n-M), s_Q(n), \ldots, s_Q(n-M)\right) \end{aligned} \tag{5}$$

Focused Time-Delay Neural Network (FTDNN) [15] is one of the simplest neural networks that incorporates memory effects. The memory effects are modeled by using delayed input samples, where means one sample delay. Here real-valued version of FTDNN is employed, i.e., weights, biases, activation functions, and outputs are all real-valued.

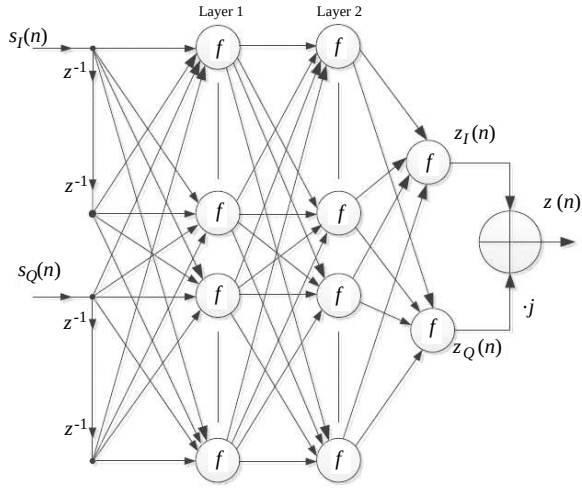

Figure 2. RSFTDNN model.

Since the final output is complex, the model should also have double-output — one for real part, the other for imaginary. This turns out to be a double-vector-input double-output (DVIDO) neural network, or in scalar form $2\,(M\,+\,1)$-input-double-output neural network.

Figure 2 shows the structure, which has 2 layers. The complex signal is in the form:

$$s(n) = s_I(n) + js_Q(n) \tag{6}$$

where the I path signal $s_I(n)$ represents the real part, while the Q path signal $s_Q(n)$ represents the imaginary part. Hence the proposed neural network is named *rectangular structured Focused Time-Delay Neural Network* model.

Let $x_{i,(l+1)}(n)$ denote the output of the ith neuron in the $l+1$th layer. To simplify the representation, the time sample index n is ignored. The number of neurons in the lth layer is denoted as $N_{(l)}$. Then the outputs of $l+1$th layer are generated from the outputs of the lth layer by the following mathematical relation:

$$x_{i,(l+1)}(n) = \Phi_{i,(l+1),PA}\left(\sum_{j=1}^{N_{(l)}} \alpha_{ij,(l+1)} x_{j,(l)}(n) + \beta_{i,(l+1)}\right) \tag{7}$$

where $\Phi_{i,(l+1),PA}(\cdot)$ is called the activation function for the ith neuron in the $l+1$th layer. $\alpha_{ij,(l+1)}$ is the weights from the jth neuron in the lth layer to the ith neuron in the $l+1$th layer, and $\beta_{i,(l+1)}$ is the bias for the ith neuron in the $l+1$th layer.

To further simplify the network, all the inner activation functions and the output layer activation function are the same, denoted as $f(\cdot)$. Note that the AM/AM relationship is a "bend-down" curve, i.e., the slope of the curve is decreasing with increasing input amplitude. To reflect this inherent "bend-down" nature of power amplifier distortion, the activation function is chosen to be a *sigmoid* function, which also bends down for large input. The Sigmoid function is given by:

$$f_{sgm}(x) = \frac{2c_1}{1 + e^{-c_2 \cdot x}} - c_1 \tag{8}$$

And its *1st*-order derivative function is

$$f'_{sgm}(x) = \frac{c_2}{2c_1}\left(c_1^2 - f_{sgm}^2(x)\right) \tag{9}$$

where parameter c_2 is the slope parameter, and c_1 defines the range of sigmoid function as $(0,\ c_1]$. The identification method used is the well-known back-propagation (BP) method [14].

4. EXPERIMENT RESULTS

4.1. Experiment Setup

Figure 3 shows the overall experimental setup. The device-under-model (DUM) consists of the vector signal generator and the power amplifier (PA). Specifically, the signal generator contains TX IQ imbalances distortion, while power amplifier contains the nonlinear

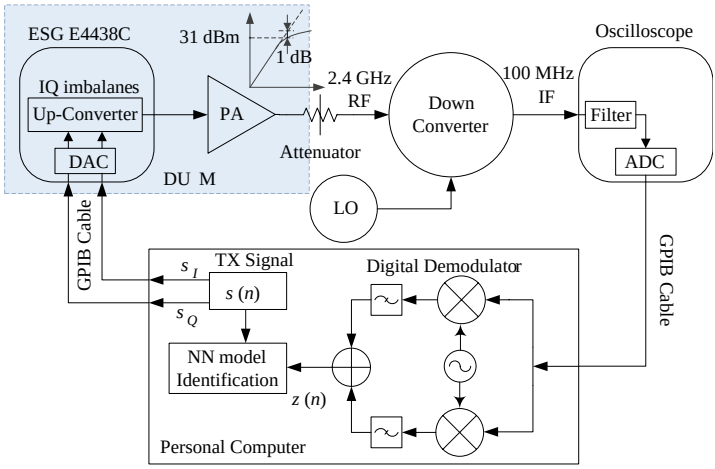

Figure 3. Experiment devices setup diagram.

and memory PA distortion. Here the signal generator is Agilent ESG E4438C vector signal generator, which consists of the I-Path/Q-Path DACs, the reconstruction filters and the up-converters, as well as other analog devices. And the power amplifier is Mini-Circuits ZVE-8G Amplifier.

The training signal is complex white uniform distributed random signal. It is to uniformly sample and explore the meaningful range of the mathematical model of the DUM, and give equal weight to different amplitude. The digital baseband training signal is passed to the signal generator (ESG E4438C). Then the signal generator (ESG E4438C) converts the digital baseband signal to its corresponding RF signal by passing it through the I-Path/Q-Path DACs, the reconstruction filters and the up-converters, where the generated RF signal has carrier frequency of 2.4 GHz and bandwidth of 16.6 MHz. After that, the signal passes through the power amplifier (PA), with the average output power of around 31 dBm that is also the 1 dB gain compression point. In the receiver, the RF signal is first down-converted to an intermediate frequency (IF) signal of 100 MHz by the down converter, and then received and digitized by the oscilloscope (Infiniium 54832D DSO) with sampling rate of 2 Gsps. The digital signal is then passed to the personal computer (PC). The digital IF signal is further down-converted to baseband by the digital demodulator, which prevents the signal from additional RX IQ imbalances distortion. After time alignment, the received baseband signal and the transmitted signal are used to identify the RSFTDNN model.

Totally 42,818 pairs of input-output data samples are used. Following the work of Doyle et al. [16] of using 50% of samples for model identification and 50% for model verification, the first 50% of the dataset (21,409 pairs) is used to train the RSFTDNN model, while the remaining 50% of the dataset (21,409 pairs) is used for testing. As a criterion, the normalized root mean square error (NRMSE) is used to evaluate the performance and accuracy of the model:

$$NRMSE = \sqrt{\frac{\sum_{n=1}^{N} |s(n) - z(n)|^2}{\sum_{n=1}^{N} |s(n)|^2}} \tag{10}$$

where N is the number of testing samples.

For comparison, the performance of the memory polynomial model (MPM) based dual input model [17] is also evaluated. Note that memory polynomial model [18] is a typical polynomial based model and one of the simplest versions of the Volterra based model. Hence it

is supposed to have the least condition number problem and consume the least computation resources among polynomial based models. Its nonlinear order is set to be 5, the same as in [17].

4.2. RSFTDNN Model of TX IQ Imbalances and PA Distortions

The TX IQ imbalances distortion caused by the circuits inside the signal generator and power amplifier are modeled by the RSFTDNN model. The memory depth is 20, i.e., there are 20 delay taps at the input. And there are 2 inner layers, and 1 output layer. Each inner layer has 10 neurons, with Sigmoid activation function. There are 2 neurons in the output layer, and hence two outputs of the RSFTDNN model — one for I component, the other for Q component. After complex-addition as shown in Figure 2, the final output is obtained.

The learning curve of the RSFTDNN model converges after around 5,000 iterations by setting the update step-size u as 0.01. Important physical parameters of the RF system are given in Table 1. The time domain waveform comparison is shown in Figure 4(a). Here the RSFTDNN model output waveform is compared with the

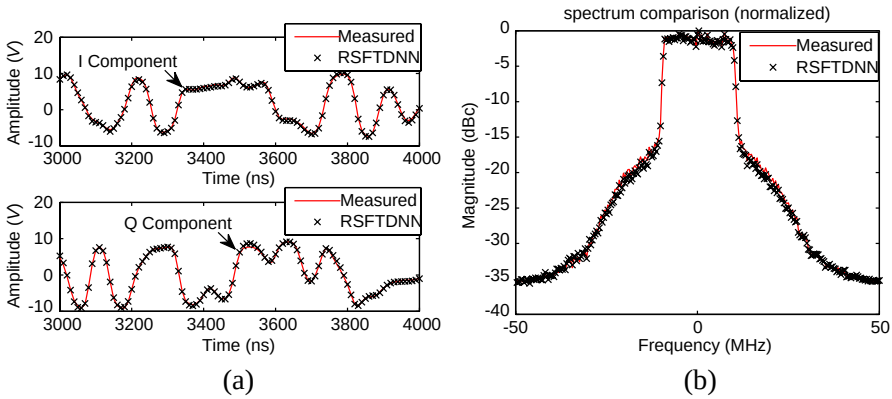

Figure 4. Time domain and spectrum comparison. (a) Time domain waveform comparison. (b) Spectrum comparison.

Table 1. Physical parameters comparison between real device and RSFTDNN model (RM), where "o-pwr" stands for "output power".

device o-pwr	31.37 dBm	device PAE	12.7%	device gain	31.36 dB
RM o-pwr	31.42 dBm	RM PAE	12.8%	RM gain	31.41 dB

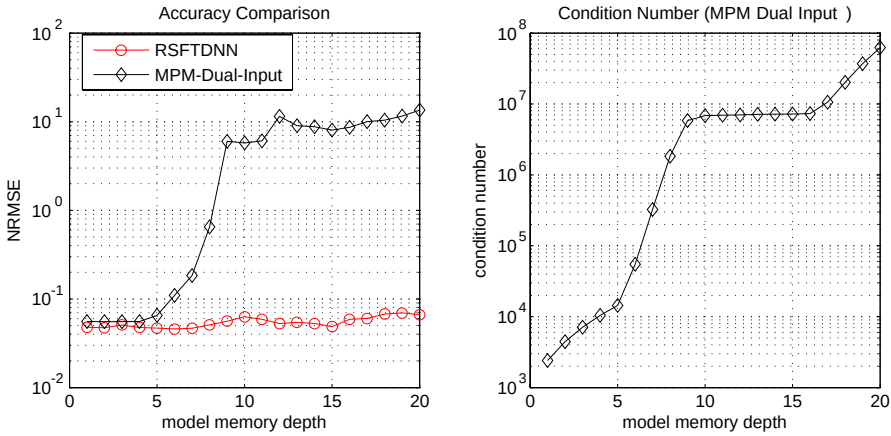

Figure 5. Accuracy comparison between RSFTDNN model and MPM-Dual-Input model, and the condition number of MPM-Dual-Input model.

measured waveform in the real experiment. I component waveform and Q component waveform are compared separately. The spectrum comparison is also shown in Figure 4(b), where the spectrum of the RSFTDNN model output is compared with the real signal in the measurement. Both figures demonstrate a good agreement between measured signal and the simulated signal by the RSFTDNN model, and justify the high accuracy of RSFTDNN model.

The accuracy of the RSFTDNN model is further compared with that of the MPM-Dual-Input model. Here the memory depths of both models are swept from 1 to 20 taps, and the accuracies of both models are compared using the NRMSE defined in Equation (10). As shown in Figure 5, the accuracy of the RSFTDNN model does not change much when the memory depth is changed, but the accuracy of MPM-Dual-Input model drops dramatically with increased memory depth. The reason for the accuracy degradation of MPM-Dual-Input model is due to the condition number problem — the condition number is increasing very fast with memory depth, which is also illustrated in Figure 5. Note that the maximum number of parameters of MPM-Dual-Input model is 252 for the case of 20 memory-tap depth. Comparing with the number of training samples (21,409 samples), the possibility of severe over-fitting problem [19] can be dismissed.

The resources required for the simulator between RSFTDNN model and MPM-Dual-Input model are compared in Figure 6. 21,409 input samples are injected into the model, and the output is calculated

and generated accordingly. The results show that RSFTDNN consume less memory space than MPM-Dual-Input and the gap increases with the model memory depth. For the case of 20 taps, RSFTDNN consumes less than 1/5 of the memory space that MPM-Dual-Input consumes. The simulation time for RSFTDNN remains relatively constant with increase in memory depth, whereas it increases 650% for the MPM-Dual-input when the memory depth increases from 1-tap to 20-taps. In absolute simulation time, the RSFTDNN has an advantage over MPM-Dual-Input for memory depth beyond 11 taps.

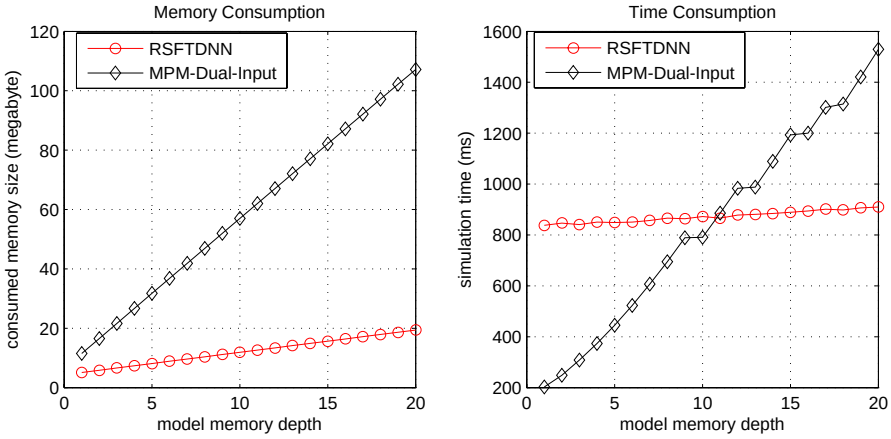

Figure 6. Resources consumption comparison between RSFTDNN model and MPM-Dual-Input model: memory space consumption and simulation time consumption. The comparison is based on a Hewlett-Packard Z210 workstation with Intel Xeon CPU E31225 @3.10 GHz and 4.00 GB RAM memory.

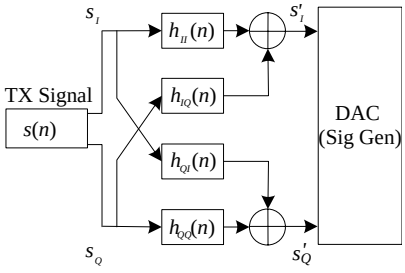

Figure 7. Additional IQ imbalances added in baseband

4.3. Effect of Increased IQ Imbalances

To simulate a low cost vector modulator that has poor IQ imbalances, additional IQ imbalances are added onto the inherent IQ imbalances in the signal generator. It is added onto the transmitted signal $s(n)$. In order to enhance the memory effects of the distortion, the additional IQ imbalances are implemented by four linear filters, as shown in Figure 7. The four low pass filters h_{II}, h_{IQ}, h_{QI}, h_{QQ} are used to model the TX IQ imbalances distortion, with memory effects and cross-talking between I and Q paths. Their coefficients are given in Table 2. The original transmit signal $s(n)$ is firstly distorted by the IQ imbalances model. After that, the newly distorted signal $s'(n)$ is passed to the signal generator and the whole transmission channel, where it further suffers from TX IQ imbalances and PA distortions in the physical device.

The RSFTDNN model has the same structure as in the previous case. With the update step-size u being set 0.01, the learning curve converges after 5,000 iterations. Important physical parameters of

Table 2. Coefficients of the four low pass filters h_{II}, h_{IQ}, h_{QI}, h_{QQ}.

h_{II}	0.0021, 0.0734, 0.1546, 0.219, 0.2435, 0.219, 0.1546, 0.0734, 0.0021
h_{IQ}	0.0006, 0.0026, 0.005, 0.0072, 0.0085, 0.0085, 0.0072, 0.005, 0.0026
h_{QI}	0.0008, 0.0028, 0.0051, 0.0068, 0.0074, 0.0068, 0.0051, 0.0028, 0.0008
h_{QQ}	0.0024, 0.0737, 0.155, 0.2195, 0.2441, 0.2195, 0.155, 0.0737, 0.0024

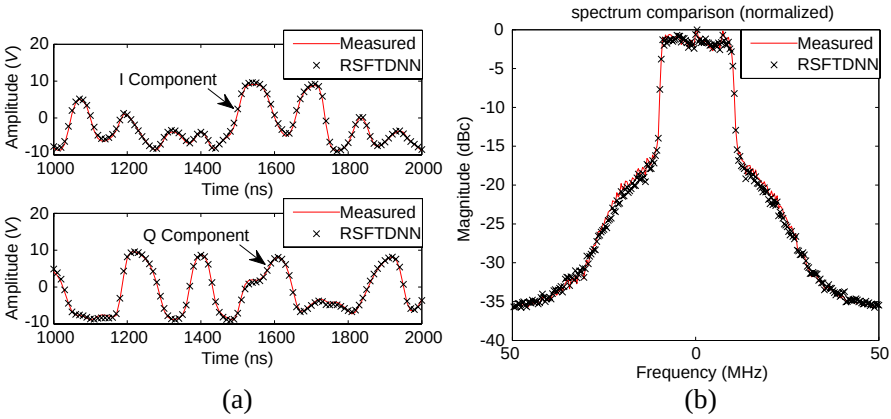

Figure 8. Time domain and spectrum comparison. (a) Time domain waveform comparison. (b) Spectrum comparison.

the RF system are given in Table 3. Time domain waveform of the RSFTDNN model is compared with the measured signals in Figure 8(a), where each I and Q components are compared separately. The spectrum comparison is shown in Figure 8(b). Both these comparisons show that the RSFTDNN model is very accurate, and the simulated output of the model is in good agreement with the measured signal.

The accuracy of the RSFTDNN model is also compared with that of the MPM-Dual-Input model, with the memory depths of both models being swept from 1 to 20 taps, as illustrated in Figure 9. As in the previous case, the accuracy of RSFTDNN model does not change much when the memory depth is changed. On the contrary, owing to the fast-growing condition number, also illustrated in Figure 9, the accuracy of the MPM-Dual-Input model is deteriorating very fast with increased memory depth. The resources required for the simulator of 21,409 input samples between RSFTDNN model and MPM-Dual-Input model are compared in Figure 10.

Table 3. Physical parameters comparison between real device and RSFTDNN model (RM), where "o-pwr" stands for "output power".

device o-pwr	31.36 dBm	device PAE	12.7%	device gain	31.35 dB
RM o-pwr	31.50 dBm	RM PAE	13.1%	RM gain	31.49 dB

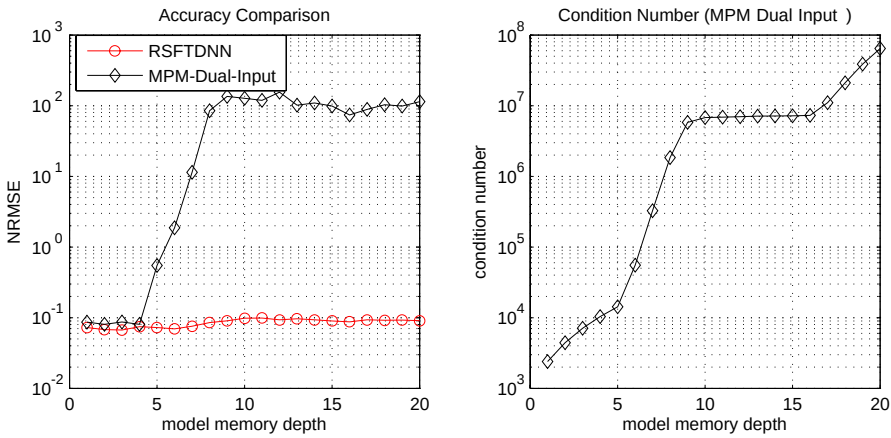

Figure 9. Accuracy comparison between RSFTDNN model and MPM-Dual-Input model, and the condition number of MPM-Dual-Input model.

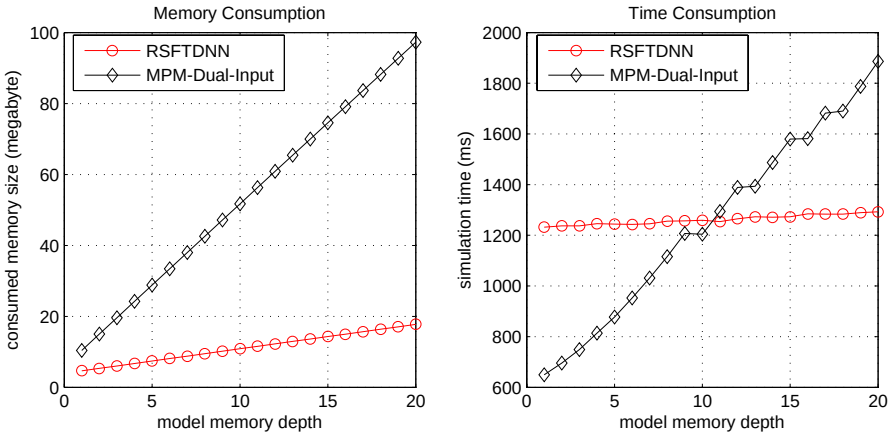

Figure 10. Resources consumption comparison between RSFTDNN model and MPM-Dual-Input model: memory space consumption and simulation time consumption. The comparison is done based on the same computer as the previous experiment.

5. CONCLUSION

RSFTDNN model is proposed to unify and model the behavior of the TX IQ imbalances and power amplifier. It saves computation resources in system-level simulation, provides unified view of the transmitter system, and can be conveniently implemented in experiment. The RSFTDNN model successfully overcome the condition number problem in polynomial based models, and can accurately characterize both mild and deep nonlinear system. Its structure is simple to implement, and is stable because there is no feedback loop. The model is tested on a transmitter with IQ imbalance and the power amplifier operated into gain compression mode.

Results show very good agreement between measured and modeled in time domain waveform and the transmitted spectrum. Compared with the dual input memory polynomial model, the RSFTDNN model uses less resources and is more accurate.

REFERENCES

1. Emami, S., P. Hajireza, F. Abd-Rahman, H. Abdul-Rashid, H. Ahmad, and S. Harun, "Wide-band hybrid amplifier operating in S-band region," *Progress In Electromagnetics Research*, Vol. 102, 301–313, 2010.

2. Raab, F., P. Asbeck, S. Cripps, P. Kenington, Z. Popovic, N. Pothecary, J. Sevic, and N. Sokal, "RF and microwave power amplifier and transmitter technologies — Part 1," *High Frequency Electronics*, Vol. 2, No. 3, 22–36, 2003.
3. Thein, T., C. Law, and K. Fu, "Frequency domain dynamic thermal analysis in GaAs Hbt for power amplifier applications," *Progress In Electromagnetics Research*, Vol. 118, 71–87, 2011.
4. Liu, T., S. Boumaiza, and F. Ghannouchi, "Deembedding static nonlinearities and accurately identifying and modeling memory effects in wide-band RF transmitters," *IEEE Transactions on Microwave Theory and Techniques*, Vol. 53, No. 11, 3578–3587, 2005.
5. Ku, H. and J. Kenney, "Behavioral modeling of nonlinear RF power amplifiers considering memory effects," *IEEE Transactions on Microwave Theory and Techniques*, Vol. 51, No. 12, 2495–2504, 2003.
6. Wulich, D., "Definition of efficient PAPR in OFDM," *IEEE Communications Letters*, Vol. 9, No. 9, 832–834, 2005.
7. Ding, L., Z. Ma, D. Morgan, M. Zierdt, and G. T. Zhou, "Compensation of frequency-dependent gain/phase imbalance in predistortion linearization systems," *IEEE Transactions on Circuits and Systems I: Regular Papers*, Vol. 55, No. 1, 390–397, 2008.
8. Narasimhan, B., D. Wang, S. Narayanan, H. Minn, and N. Al Dhahir, "Digital compensation of frequency-dependent joint Tx/Rx I/Q imbalance in OFDM systems under high mobility," *IEEE Journal of Selected Topics in Signal Processing*, Vol. 3, No. 3, 405–417, 2009.
9. Anttila, L., P. Handel, and M. Valkama, "Joint mitigation of power amplifier and I/Q modulator impairments in broadband directconversion transmitters," *IEEE Transactions on Microwave Theory and Techniques*, Vol. 58, No. 4, 730–739, 2010.
10. Rugh, W., *Nonlinear System Theory*, Johns Hopkins University Press, Baltimore, MD, 1981.
11. Gharaibeh, K., O. Al-Zoubi, and A. Alzayed, "Adaptive predistortion using threshold decomposition-based piecewise linear modeling," *International Journal of RF and Microwave Computer-Aided Engineering*, Vol. 21, No. 2, 145–156, 2011.
12. Rawat, M., K. Rawat, and F. Ghannouchi, "Adaptive digital predistortion of wireless power amplifiers/transmitters using dynamic real-valued focused time-delay line neural networks," *IEEE Transactions on Microwave Theory and Techniques*, Vol. 58,

No. 1, 95–104, 2010.

13. Heath, M., *Computing: An Introductory Survey*, McGraw-Hill, 1998.
14. Haykin, S., *Adaptive Filter Theory*, Prentice-Hall, 1996.
15. Htike, K. and O. Khalifa, "Rainfall forecasting models using focused time-delay neural networks," *2010 IEEE International Conference on Computer and Communication Engineering (ICCCE)* 1–6, 2010.
16. Doyle, F., R. Pearson, and B. Ogunnaike, *Identification and Control Using Volterra Models*, Springer Verlag, 2002.
17. Cao, H., A. Tehrani, C. Fager, T. Eriksson, and H. Zirath, "Dual-input nonlinear modeling for I/Q modulator distortion compensation," *IEEE Radio and Wireless Symposium, RWS' 09*, 39–42, 2009.
18. Kim, J. and K. Konstantinou, "Digital predistortion of wideband signals based on power amplifier model with memory," *Electronics Letters*, Vol. 37, No. 23, 1417–1418, 2001.
19. Bridewell, W., N. Asadi, P. Langley, and L. Todorovski, "Reducing overfitting in process model induction," *Proceedings of the 22nd International Conference on Machine Learning, ACM*, 81–88, 2005.